

Available online at [www.sciencedirect.com](http://www.sciencedirect.com)

**jmr&t**  
Journal of Materials Research and Technology  
[www.jmrt.com.br](http://www.jmrt.com.br)



## Original Article

# Thermodynamic modeling of phases equilibrium in aqueous systems to recover potassium chloride from natural brines



Ruberlan Gomes da Silva<sup>a,\*</sup>, Marcelo Seckler<sup>b</sup>, Sonia Denise Ferreira Rocha<sup>c</sup>, Daniel Saturnino<sup>d</sup>, Éder Domingos de Oliveira<sup>d</sup>

<sup>a</sup> Mineral Development Centre of Vale, Santa Luzia, MG, Brazil

<sup>b</sup> Department of Chemical Engineering, Universidade de São Paulo (USP), São Paulo, SP, Brazil

<sup>c</sup> Department of Mining Engineering, Universidade Federal de Minas Gerais (UFMG), Belo Horizonte, MG, Brazil

<sup>d</sup> Department of Chemical Engineering, Universidade Federal de Minas Gerais (UFMG), Belo Horizonte, MG, Brazil

## ARTICLE INFO

## Article history:

Received 9 November 2015

Accepted 17 May 2016

Available online 11 June 2016

## Keywords:

Quinary system

Natural brine

Potassium chloride

Pitzer and Harvie's model

Fractional crystallization

## ABSTRACT

Chemical fertilizers, such as potassium chloride, ammonium nitrate and other chemical products like sodium hydroxide and soda ash are produced from electrolyte solutions or brines with a high content of soluble salts. Some of these products are manufactured by fractional crystallization, when several salts are separated as solid phases with high purity (>90%). Due to the large global demand for potassium fertilizers, a good knowledge about the compositions of salts and brines is helpful to design an effective process. A thermodynamic model based on Pitzer and Harvie's model was used to predict the composition of crystallized salts after water removal by forced evaporation and cooling from multicomponent solutions or brines. Initially, the salts' solubilities in binary systems (NaCl–H<sub>2</sub>O, KCl–H<sub>2</sub>O and MgCl<sub>2</sub>–H<sub>2</sub>O) and ternary system (KCl–MgCl<sub>2</sub>–H<sub>2</sub>O) were calculated at 20 °C and compared with literature data. Next, the model was compared to our experimental data on the quinary system NaCl–KCl–MgCl<sub>2</sub>–CaCl<sub>2</sub>–H<sub>2</sub>O system at 20 °C. The Pitzer and Harvie's model represented well both the binary and ternary systems. Besides, for the quinary system the fit was good for brine densities up to 1350 kg/m<sup>3</sup>. The models were used to estimate the chemical composition of the solutions and salts produced by fractional crystallization and in association with material balance to respond to issues related to the production rates in a solar pond containing several salts dissolved, for instance, NaCl, KCl, MgCl<sub>2</sub> and CaCl<sub>2</sub>.

© 2016 Brazilian Metallurgical, Materials and Mining Association. Published by Elsevier Editora Ltda. This is an open access article under the CC BY-NC-ND license (<http://creativecommons.org/licenses/by-nc-nd/4.0/>).

\* Corresponding author.

E-mail: [ruberlan.silva@vale.com](mailto:ruberlan.silva@vale.com) (R.G.d. Silva).

<http://dx.doi.org/10.1016/j.jmrt.2016.05.006>

2238-7854/© 2016 Brazilian Metallurgical, Materials and Mining Association. Published by Elsevier Editora Ltda. This is an open access article under the CC BY-NC-ND license (<http://creativecommons.org/licenses/by-nc-nd/4.0/>).

## 1. Introduction

The solubility prediction of electrolytes in aqueous solutions is essential for a variety of processes such as brines and seawater desalination, drowning-out crystallization as well as liquid-liquid extraction in chemical, mineral and hydrometallurgical industries [1]. For example, solar evaporation is applied to brine ponds in northern regions of Argentina and Chile to produce saleable salts like potassium chloride, potassium sulphate and lithium salts [2]. The process is based on fractional crystallization [3], which provides separation of inorganic salts with purities compatible with market requirements. Thermodynamic models are useful tools to estimate the solution composition during crystallization, which is needed for reliable industrial process design. In this context, Pitzer's ion-interaction model and its extended Harvie and Weare's model [4-6] are suitable tools because they are reliable for predicting salt's solubility in multicomponent aqueous systems with high ionic strength over a wide range of temperatures (0-300 °C) [7-9]. Considering this, it is the objective of this study to analyze the technical feasibility of recovering potassium chloride from a natural complex brine, here represented as the quinary system NaCl-KCl-MgCl<sub>2</sub>-CaCl<sub>2</sub>-H<sub>2</sub>O. Given the lack of information for such quinary system, experimental data on solubilities have been determined and compared to Pitzer's ion-interaction model predictions. The validated model has been used to develop a technically feasible fractional crystallization process.

## 2. Material and methods

Batch crystallization experiments with a natural brine from a dry salt lake located at the north of Argentina were performed in a 2 l jacketed glass crystallizer. Temperature was controlled by an electric heating system at 85 ± 3 °C. A mechanic stirrer at 250 RPM provided mixing, using a 45° pitched blade impeller. Table 1 shows the chemical composition of the natural brine under investigation.

The natural brine sample was distributed in four recipients and concentrated by forced evaporation at 85 °C at ambient pressure (~1 atmosphere). Thereafter, the pulps were cooled to 20 °C to increase yield and kept under stirring for 24 h at 250 RPM in order to achieve equilibrium. The initial brine (1.198 g/cm<sup>3</sup> at 20 °C) was concentrated up to 1.250 g/cm<sup>3</sup> at 20 °C, which is now called the Step 1 in this methodology. The solid and liquid phases in equilibrium were then separated by vacuum filtration. The liquid phase with 1.250 g/cm<sup>3</sup> was subjected to another cycle of evaporation at 85 °C followed by a cooling process to 20 °C in order to increase its density to 1.304 g/cm<sup>3</sup> at 20 °C and this is the Step 2. The crystallization and solids separation procedures were repeated two

more times to produce brines with densities of 1.354 g/cm<sup>3</sup> at 20 °C in Step 3 and 1.427 g/cm<sup>3</sup> at 20 °C in Step 4. The evaporation at 85 °C is required to concentrate the brine samples to desired densities in a timely manner and then cooling to 20 °C. The temperature of 20 °C was chosen because it is the average brine temperature processed in dry salt lakes, like Salar de Atacama in Chile [2]. The less soluble and more abundant salts, for example NaCl, crystallized at the beginning of the process, whereas the more soluble and less abundant ones (CaCl<sub>2</sub>·MgCl<sub>2</sub>·12H<sub>2</sub>O) crystallized at the end of the experiment. Sodium, potassium, magnesium, calcium and chloride contents in solution were analyzed as well as in the wet salts obtained in each step.

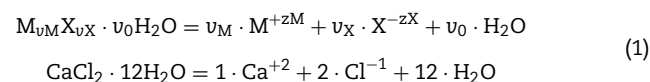
The solutions were diluted and the respective wet salts dissolved in doubly deionized water to determine the sodium, potassium, magnesium and calcium contents by PerkinElmer NexION 200D ICP-MS. The chloride concentrations in the liquid and solid phases were determined by titration with a standard solution of AgNO<sub>3</sub> in the presence of drops of 0.1% (w/v) K<sub>2</sub>CrO<sub>4</sub> as an indicator.

Samples for X-ray diffraction were ground below 200 # TYLER MESH (0.074 mm) and analyzed on PANalytical Model X'PERT PRO MPD (PW 3419) with PW3050/60 (θ/θ) goniometer, X-ray ceramics tubes, anode of Cu (Kα<sub>1</sub> = 1.540598 Å) and PW3373/00 model (2000 W-60 kV). Diffraction patterns were acquired from 5° to 75°2θ at 0.02 steps. The identification of all minerals was done with X'Pert HighScore version 2.1b software from PANalytical.

## 3. Results and discussion

The solubility equilibrium constant,  $K_{sp}$ , at a fixed temperature and pressure for the dissolution reaction of hydrated salt ( $M_{\nu_M}X_{\nu_X} \cdot \nu_0 H_2O$ ), having  $\nu_M$  positive ions (M), of charge  $z_M$ , and  $\nu_X$  negative ions (X) of charge  $z_X$ , as well  $\nu_0$  molecules of water (Eq. (1)) [8] is expressed by Eq. (2) [8]:

Example:



$$\ln K_{sp} = - \left[ \frac{(\nu_M \cdot \mu^\circ_M + \nu_X \cdot \mu^\circ_X + \nu_0 \cdot \mu^\circ_{H_2O})}{R \cdot T} \right] + \left[ \frac{(\mu^\circ_S)}{R \cdot T} \right] \quad (2)$$

where  $\mu^\circ$  is the standard chemical potential of solids ( $\mu^\circ_S$ ), water ( $\mu^\circ_{H_2O}$ ) and for the ions solution ( $\mu^\circ_M$  and  $\mu^\circ_X$ ) at a given temperature (T) and R is the gas universal constant. The standard state for the aqueous ions and electrolytes was taken to be a hypothetical one molal solution referenced to infinite dilution at any pressure and temperature. The solid

**Table 1 – Density and chemical composition of the natural brine.**

Density at 20 °C (g/cm <sup>3</sup> )	NaCl (g/L)	KCl (g/L)	MgCl <sub>2</sub> (g/L)	CaCl <sub>2</sub> (g/L)	CaSO <sub>4</sub> (g/L)	Total salts (g/L)
1.198	244.17	17.20	28.20	58.50	0.19	348.26

and solvent standard states were taken to be the respective pure phases at the pressure and temperature of interest.

The saturation index (SI) for KCl is expressed by the ratio between the ionic product (IP) and the solubility product according Eq. (3) [10]. In terms of the activities, the ionic product is given by Eq. (4) [10].

$$SI_{KCl} = \frac{IP(KCl)}{K_{sp}(KCl)} \quad \text{and} \quad \frac{IP(M_{vM}X_{vX} \cdot \nu_0 H_2O)}{K_{sp}(M_{vM}X_{vX} \cdot \nu_0 H_2O)} \quad (3)$$

$$IP(KCl) = a_{K^+} \cdot a_{Cl^-} \quad \text{and} \quad IP(M_{vM}X_{vX} \cdot \nu_0 H_2O) \\ = (a_{M^{+zM}})^{\nu_M} \cdot (a_{X^{-zX}})^{\nu_X} \cdot (a_{H_2O})^{\nu_0} \quad (4)$$

where  $a_{K^+} = m_{K^+} \cdot \gamma_{K^+}$  for the potassium chloride case, but for a generic cation the equation becomes  $a_{M^{+zM}} = m_{M^{+zM}} \cdot \gamma_{M^{+zM}}$ . For the anion, the KCl case becomes  $a_{Cl^-} = m_{Cl^-} \cdot \gamma_{Cl^-}$  and for a generic anion  $a_{X^{-zX}} = m_{X^{-zX}} \cdot \gamma_{X^{-zX}}$ . Furthermore,  $a_i$  is the ionic activity,  $m_i$  the molal concentration and  $\gamma_i$  the activity coefficient, for single ions, where  $i = K^+$ ,  $Cl^-$ ,  $M^{+zM}$  or  $X^{-zX}$ .

The activity coefficients ( $\gamma_i$ ) are calculated by the Pabalan and Harvie's model according to the literature [5,8]. With these values, it is possible to calculate the IP for a specific salt at a specific temperature. The SI is calculated since the  $K_{sp}$  is known from the literature. If  $SI = 1$  the solution is saturated, if  $SI < 1$  the solution is unsaturated and if  $SI > 1$  the solution is supersaturated. The activity of water ( $a_{H_2O}$ ) is related to the osmotic coefficient,  $\phi$ , by Eq. (5) [8].

$$a_{H_2O} = \exp \left( -\phi \cdot \frac{\sum m_i \cdot 18}{1000} \right) \quad (5)$$

where  $\sum m_i$  is the sum of molalities of species in solution. The osmotic coefficient,  $\phi$ , is calculated from ion-interactions [8].

In order to check the results obtained by Pabalan and Harvie's model [5,8], the solubilities in selected binary systems were calculated and compared with data from Pabalan and

Pitzer [8]. Fig. 1a and b shows that the molalities calculated by the Pitzer and Harvie's model [5,8] fit well with experimental measurements obtained by Pabalan and Pitzer [5] for the binary systems NaCl-H<sub>2</sub>O, KCl-H<sub>2</sub>O and MgCl<sub>2</sub>-H<sub>2</sub>O at different temperatures and for the ternary system NaCl-KCl-H<sub>2</sub>O at 20 °C.

Experimentally determined equilibrium compositions of brines at 20 °C with the respective solids are shown in Tables 2 and 3. It is observed that the pH decreases from 7.4 to 2.1 from Step 1 to Step 4, corresponding to a brine with 528 g/L of salts, mainly calcium chloride (29.77% w/w).

The calculated compositions by the Pitzer and Harvie's model [5,8] of the equilibrium brines at 20 °C are given in Table 4. Fig. 2a and b shows a comparison between the compositions of equilibrium brines at 20 °C predicted by the model and the experimental values obtained in the present work.

Tables 2 and 3 show that in Step 1, after the reduction of about 59% of total initial free water, only NaCl and CaSO<sub>4</sub> crystallize in the solid phase, with a composition of 99.9% w/w of NaCl and 0.10% w/w of CaSO<sub>4</sub>. The content of water reduced in the brine due to the amount of water evaporated and the amount of water of crystallization in the salts. The concentration of all salts, excluding NaCl and CaSO<sub>4</sub>, increased as the brine density is raised from 1.198 g/cm<sup>3</sup> to 1.250 g/cm<sup>3</sup> both measured at 20 °C. The brine pH decreased from 7.4 to 6.5. The overflow brine from Step 1 became saturated in KCl and the total soluble salts increased from 348 to 381 g/L.

The brine produced after Step 2, followed by a reduction of about 74% of total initial free water, showed the formation of NaCl and KCl crystals. The salt had a composition of 62.8% w/w of NaCl and 37.2% w/w of KCl. The concentration of all salts, discounting NaCl, increased as the brine density grew up from 1.250 g/cm<sup>3</sup> to 1.304 g/cm<sup>3</sup> measured at 20 °C. The brine pH decreased from 6.5 to 5.5. The brine became saturated for carnallite salt. The total soluble salts solids increased from 381 to 473 g/L.

In Step 3 after evaporation of 85% of total initial free water, NaCl, KCl, KCl·MgCl<sub>2</sub>·6H<sub>2</sub>O and a small amount of

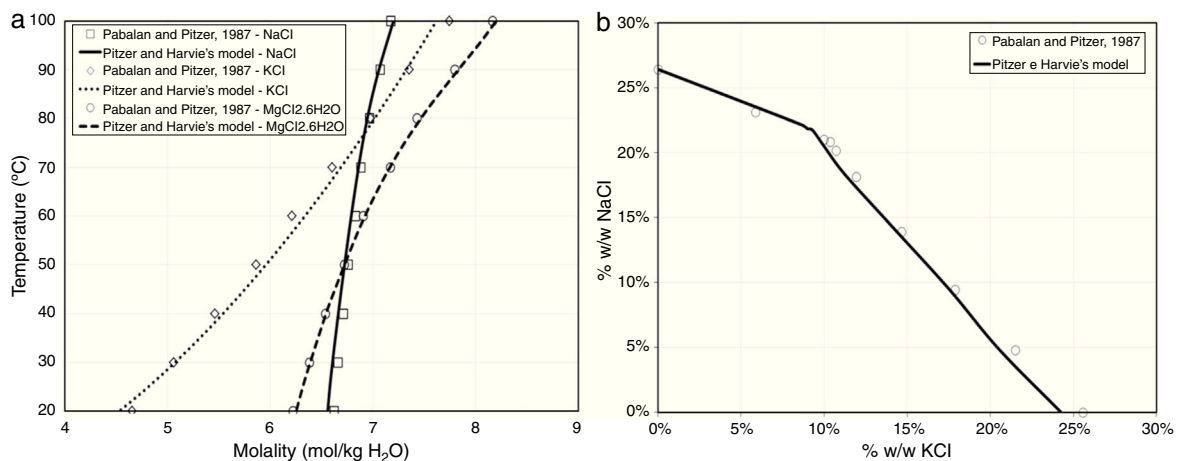


**Fig. 1 – Comparison between solubilities obtained by Pitzer and Harvie's model [5,8] and experimental data from Pabalan and Pitzer [5] for (a) the binaries systems NaCl-H<sub>2</sub>O, KCl-H<sub>2</sub>O and MgCl<sub>2</sub>-H<sub>2</sub>O at various temperatures and (b) the ternary system NaCl-KCl-H<sub>2</sub>O at 20 °C.**

**Table 2 – Experimental solubility data NaCl–KCl–MgCl<sub>2</sub>–CaCl<sub>2</sub>–H<sub>2</sub>O system at 20 °C with natural brine.**

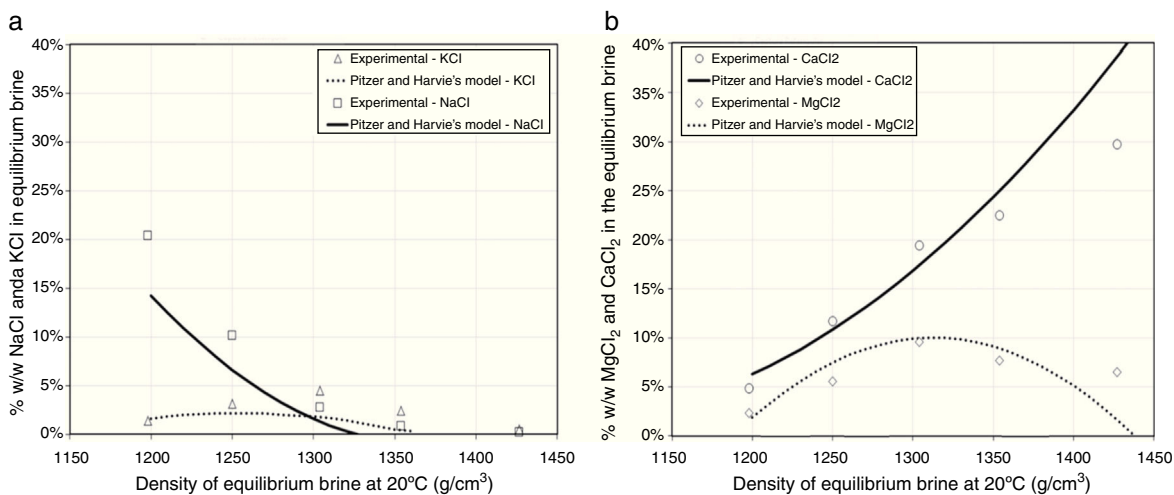
Step of forced evaporation	Density at 20 °C (g/cm <sup>3</sup> )	% w/w evaporated water	Liquid phase composition (%w/w)						pH	Total solids dissolved (g/L)
			NaCl	KCl	MgCl <sub>2</sub>	CaCl <sub>2</sub>	CaSO <sub>4</sub>	H <sub>2</sub> O		
Feed <sup>(a)</sup>	1.198	0	20.38	1.44	2.35	4.88	0.02	70.93	7.4	348
Step 1	1.250	59	10.07	3.19	5.55	11.69	0.01	69.49	6.5	381
Step 2	1.304	74	2.76	4.47	9.58	19.47	0.00	63.72	5.5	473
Step 3	1.354	85	0.85	2.44	7.73	22.49	0.15	66.49	4.3	454
Step 4	1.427	98	0.24	0.49	6.51	29.77	0.00	62.99	2.1	528

<sup>a</sup> Saturated in NaCl and CaSO<sub>4</sub>.**Table 3 – Salt composition of NaCl–KCl–MgCl<sub>2</sub>–CaCl<sub>2</sub>–H<sub>2</sub>O system at 20 °C with natural brine.**

Step of forced evaporation	Composition of solid phases (%w/w)					Solid phase identified by XRD in equilibrium with respective brine
	NaCl	KCl	MgCl <sub>2</sub>	CaCl <sub>2</sub>	CaSO <sub>4</sub>	
Feed	0	0	0	0	0	Clear Solution
Step 1	99.9	0	0	0	0.10	NaCl and CaSO <sub>4</sub>
Step 2	62.8	37.2	0	0	0	NaCl and KCl
Step 3	10.3	7.8	79.3	2.6	0	NaCl, KCl, Carnallite (KCl·MgCl <sub>2</sub> ·6H <sub>2</sub> O), Bischofite (MgCl <sub>2</sub> ·6H <sub>2</sub> O), Tacahydrate (CaCl <sub>2</sub> ·MgCl <sub>2</sub> ·12H <sub>2</sub> O) and/or Antractite (CaCl <sub>2</sub> ·2H <sub>2</sub> O)
Step 4	3.8	1.8	7.9	86.5	0	NaCl, KCl, KCl·MgCl <sub>2</sub> ·6H <sub>2</sub> O, MgCl <sub>2</sub> ·6H <sub>2</sub> O, CaCl <sub>2</sub> ·MgCl <sub>2</sub> ·12H <sub>2</sub> O and/or Antractite

**Table 4 – Brine composition for the system NaCl–KCl–MgCl<sub>2</sub>–CaCl<sub>2</sub>–H<sub>2</sub>O system at 20 °C calculated by Pitzer and Harvie's model [5,8] with natural brine.**

Feed and after forced evaporation Step	Density at 20 °C (g/cm <sup>3</sup> )	Composition of liquid phase (%w/w)						Activity of water (a <sub>w</sub> )
		NaCl	KCl	MgCl <sub>2</sub>	CaCl <sub>2</sub>	CaSO <sub>4</sub>	H <sub>2</sub> O	
Feed	1.198	15.25	1.53	2.51	5.21	0.02	75.38	0.726
Step 1	1.250	5.30	2.909	5.95	12.33	0.01	73.51	0.643
Step 2	1.304	1.33	1.14	8.96	18.58	0.00	69.99	0.509
Step 3	1.354	0.26	0.404	11.253	22.49	0.00	65.60	0.347
Step 4	1.427	0.16	0.95	0.78	39.53	0.00	58.56	0.324

**Fig. 2 – Comparison between predicted Pitzer and Harvie's model [5,8] and experimental values for the NaCl–KCl–MgCl<sub>2</sub>–CaCl<sub>2</sub>–H<sub>2</sub>O system at 20 °C: (a) NaCl and KCl, (b) MgCl<sub>2</sub> and CaCl<sub>2</sub>.**

$\text{CaCl}_2 \cdot \text{MgCl}_2 \cdot 12\text{H}_2\text{O} / \text{CaCl}_2 \cdot 2\text{H}_2\text{O}$  crystallized. The solid phase showed a composition of 10.3% w/w of NaCl, 7.8% w/w of KCl, 79.3% w/w of  $\text{MgCl}_2$  and 2.6% w/w of  $\text{CaCl}_2$ . The presence of  $\text{CaCl}_2$  and  $\text{MgCl}_2$  is due to a small quantity of brine impregnating the salts. The brine density is raised up from  $1.304 \text{ g/cm}^3$  to  $1.354 \text{ g/cm}^3$  measured at  $20^\circ\text{C}$ . The brine pH decreased from 5.5 to 4.3 and the brine reached saturation for calcium salts. The observed decrease of the total soluble salts solid from 473 to 454 g/L is not physically consistent and is probably an experimental error.

The last step of forced evaporation, Step 4, led to an evaporation of about 98% of total initial free water and NaCl, KCl,  $\text{KCl} \cdot \text{MgCl}_2 \cdot 6\text{H}_2\text{O}$ ,  $\text{CaCl}_2 \cdot \text{MgCl}_2 \cdot 12\text{H}_2\text{O}$  and  $\text{CaCl}_2 \cdot 2\text{H}_2\text{O}$  crystallized. The solid phase salts were formed by 3.8% w/w of NaCl, 1.8% w/w of KCl, 7.9% w/w of  $\text{MgCl}_2$  and 86.5% w/w of  $\text{CaCl}_2$ . The brine density went up from  $1.354 \text{ g/cm}^3$  to  $1.427 \text{ g/cm}^3$  measured at  $20^\circ\text{C}$  and the pH reached a low acidic value of 2.1. The final brine was saturated for all salts with a content of soluble salts of 528 g/L.

The simulated and experimental results for natural brine (Table 4 and Fig. 2a) with reference to 1–1 electrolytes, sodium chloride (NaCl) and potassium chloride (KCl) are in a good agreement. The systems also showed that sodium chloride crystallized in all steps and reached saturation in potassium chloride after Step 1 (39.88 g/L = 3.19% w/w, brine density of  $1.250 \text{ g/cm}^3$ ).

Table 4 and Fig. 2b display the experimental concentrations of 2–2 electrolytes, magnesium chloride ( $\text{MgCl}_2$ ) and calcium chloride ( $\text{CaCl}_2$ ), in the equilibrium brines as well as those found by the Pitzer's and Harvie's model [5,8]. In experiments with brines of densities up to  $1.350 \text{ g/cm}^3$ , it is observed a small difference between the experimental and calculated data. However, for densities above  $1.350 \text{ g/cm}^3$ , the Pitzer and Harvie's model [5,8] overpredicted the solubility values of magnesium chloride and calcium chloride.

Fig. 3 shows the X-ray diffractograms for the solids produced after each crystallization step in contact with mother liquor of densities 1.250, 1.304, 1.354 and  $1.427 \text{ g/cm}^3$  at  $20^\circ\text{C}$ . It is possible to verify the formation of salts compatible with the mineral structure of halite, sodium chloride (NaCl), for solutions of density of  $1.250 \text{ g/cm}^3$ , while potassium chloride (KCl, sylvite) crystallizes from solutions of density of  $1.304 \text{ g/cm}^3$  at

$20^\circ\text{C}$ . Potassium magnesium chloride ( $\text{KCl} \cdot \text{MgCl}_2 \cdot 6\text{H}_2\text{O}$ ) with a structure similar to carnallite was identified at a density of  $1.354 \text{ g/cm}^3$  at  $20^\circ\text{C}$ , while magnesium calcium chloride ( $\text{MgCl}_2 \cdot \text{CaCl}_2 \cdot 12\text{H}_2\text{O}$ , tachahydrate), calcium chloride dihydrate ( $\text{CaCl}_2 \cdot 2\text{H}_2\text{O}$ , anthracite), crystallized only at a density of  $1.427 \text{ g/cm}^3$  at  $20^\circ\text{C}$ . These experimentally determined crystallographic phases agreed with the Pitzer and Harvie's model [5,8] predictions.

The Pitzer's and Harvie's model [5,8] were used to simulate the process to recover saleable salts from natural brine. A solar evaporation process has been designed for the extraction of potassium chloride from brine deposits of dry salt lakes, like Salar de Atacama in northern Chile. The basic stream for the material balance around a single solar pond is shown in Fig. 4 where: (i) Leakage is the brine lost from the pond through porous dikes and floors. The quantity of leakage is usually described in kg per day and it is a function of the pond area [4]. It was assumed a leakage of  $0.011 \text{ kg/day/m}^2$ ; (ii) the water evaporated is usually expressed in mm/day or  $\text{kg/day/m}^2$ . For steps 1, 2 and 3, it was assumed 3.5, 2.8 and  $2.0 \text{ kg per day per m}^2$  of water evaporated. (iii) Entrainment is related to the brine that is lost attached to the salts deposit.

As the salt crystals grow or accumulate on the pond floor, voids are created and some brine is trapped therein. The quantity of entrainment is a function of the quantity and type of salt deposited. The entrainment is generally expressed as a weight percent of the combined salts in the deposit and correspondent entrained brine. It was assumed an entrainment loss of 15% in steps 1, 2 and 3. Salts combined to entrainment are here denominated impregnated salts.

Generally, the brine concentration throughout the solar pond is uniform and equal to the concentration in the brine that exists at each step. This observation is a key assumption for the pond material balance. It was assumed that the leakages and the exit brines have the same concentration, so these streams can be created as a single stream to simplify the material balance.

For fixed concentrations at the entrance and exit points of the pond, the material balance is represented by a system of five variables: flowrate of feeding brine, flowrate of exit brine, evaporation rate, amount and composition of salts formed and pond area. The brines and salts compositions were calculated

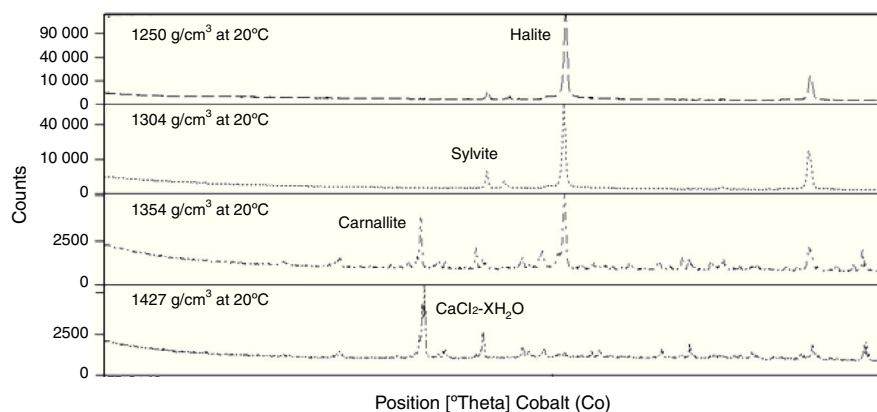


**Fig. 3 – X ray diffractograms for the crystallized salts produced after the respective equilibrium brines reach densities of 1.250, 1.304, 1.354 and  $1.427 \text{ g/cm}^3$  at  $20^\circ\text{C}$ .**

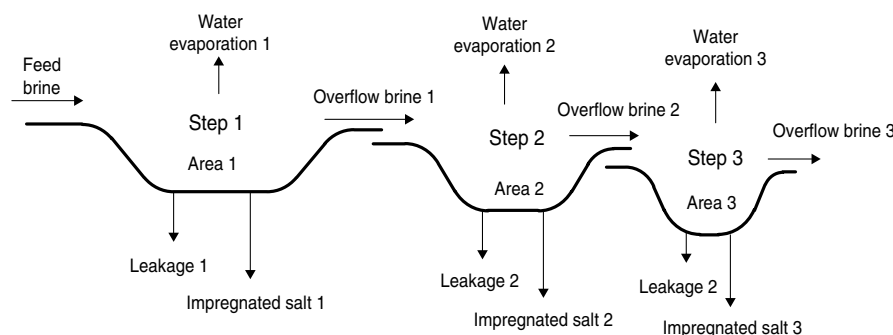


**Fig. 4 – Basic streams of a solar pond for Step 1, 2 and 3.**

by the Pitzer and Harvie's model [5,8]. Of these five variables, only two are independent. By establishing the value of any two of these variables, the system may be solved and the material balance is obtained.

The overflow brine from Step 1 feeds the Step 2 and the overflow brine from Step 2 feeds the Step 3. The overflow brine from Step 3 is called bittern brine, rich in the most soluble salts, like,  $MgCl_2$  and  $CaCl_2$ . Table 5 shows the results of the material balance for Step 1, Step 2 and Step 3 using solar evaporation process to crystallize the desired salt. Table 6 shows the composition of feed and overflow brines.

According to the solubility calculated by the Pitzer and Harvie's model [5,8] and the material balance, a sequence of three stages could lead to the crystallization of halite (87.65%w/w of NaCl) in Step 1, sylvinit (49.63% w/w

of  $NaCl + 24.31\%$  w/w of KCl) in Step 2 and a mixture of halite (5.99% w/w of NaCl), carnallite (17.46% w/w of  $KCl \cdot MgCl_2 \cdot 6H_2O$ ), bischofite (21.89% w/w of  $MgCl_2 \cdot 6H_2O$ ) and calcium chloride (47.41% w/w  $CaCl_2 \cdot 6H_2O$ ) in Step 3.

The feed brine in Step 1 is saturated in NaCl and in  $CaSO_4$ , but it is not saturated in other salts, so these are the first two salts to be crystallized. Considering the amount of evaporated water (444.77 kg/h) and an evaporation rate of 3.5 mm/day, it will be necessary a pond area of about 3050 m<sup>2</sup>. Halite crystallized in Step 1 will be harvested and fed to a NaCl Industrial Plant. The brine density at 20 °C changes from 1.198 to 1.250 g/cm<sup>3</sup>, crystallizing approximately 394 kg of halite per 1000 kg of evaporated water. Around 28% of entering potassium will be lost by impregnated brine in the salts.

**Table 5 – Material mass balance results in solar ponds.**

	Step 1	Step 2	Step 3
Pond area (m <sup>2</sup> )	3050	937	980
Feed brine (kg/h)	1000.00	378.69	231.48
Water evaporation (kg/h)	444.77	109.31	81.68
Leakage (kg/h)	1.40	0.43	0.45
Impregnated salts (kg/h)	175.14	37.47	38.20
Entrainment (kg/h)	26.27	5.62	5.73
Non impregnated salts (kg/h)	148.87	31.85	32.47
Overflow brine (kg/h)	378.69	231.48	111.15
% Accumulated evaporated water	59%	74%	85%
<i>Composition of impregnated salts (%w/w)</i>			
NaCl	76.14	45.37	7.32
KCl	2.44	22.30	5.75
$MgCl_2$	1.43	4.67	21.42
$CaCl_2$	2.96	9.69	46.86
$CaSO_4$	0.02	0.01	0.01
Total water	17.02	17.96	18.65
<i>Composition of non impregnated salts (%w/w)</i>			
NaCl	87.65	49.63	5.99
KCl	2.33	24.31	0.00
$KCl \cdot MgCl_2 \cdot 6H_2O$	0.00	0.00	17.46
$MgCl_2 \cdot 6H_2O$	1.33	7.81	21.89
$CaCl_2 \cdot 6H_2O$	1.71	10.05	47.41
$CaSO_4 \cdot 2H_2O$	0.12	0.04	0.02
Free water (% w/w)	6.88	8.16	7.23
% w/w of feed KCl crystallized (accumulated)	28	82	97
% w/w of feed KCl crystallized (in the respective Step)	28	54	15

**Table 6 – Composition of initial and overflow brines (% w/w).**

Component	Feed	Overflow Step 1	Overflow Step 2	Overflow Step 3
NaCl (%w/w)	15.35	5.30	1.33	0.26
KCl (%w/w)	1.53	2.90	1.14	0.40
MgCl <sub>2</sub> (%w/w)	2.51	5.95	8.96	11.25
CaCl <sub>2</sub> (% w/w)	5.21	12.34	18.58	22.49
CaSO <sub>4</sub> (% w/w)	0.02	0.01	0.00	0.00
Total water (% w/w)	75.39	73.50	69.99	65.61
Density at 20 °C (g/cm <sup>3</sup> )	1.198	1.250	1.304	1.354
KCl (g/L)	18.34	36.31	14.88	5.39
MgCl <sub>2</sub> (g/L)	30.07	74.33	116.78	152.27
Total soluble solids (g/L)	295	331	391	466

Saturation in KCl is achieved in the overflow brine from Step 1 that feeds Step 2 (36.31 g/L of KCl). In the solar ponds of Step 2 and Step 3, KCl-rich salts (sylvinitic and carnallite) crystallize. The sylvinitic crystallized in Step 2 is collected and fed to an industrial KCl Plant. The brine density at 20 °C changes from 1.250 to 1.304 g/cm<sup>3</sup> in Step 2, resulting in the crystallization of approximately 343 kg of salts per 1000 kg of evaporated water. About 54% of entering potassium will crystallize. Considering the amount of evaporated water in Step 2 (109.31 kg/h) and an evaporation rate of 2.8 mm/day, a pond area of about 937 m<sup>2</sup> will be necessary.

A mixture of halite, carnallite, bischofite and calcium chloride salts crystallizes in Step 3. This mixture is harvested and fed to an industrial KCl Plant as well. The brine density at 20 °C changes from 1.304 to 1.354 g/cm<sup>3</sup>, crystallizing approximately 468 kg of salts per 1000 kg of evaporated water. About 15% of entering potassium will crystallize. Considering the amount of evaporated water in Step 3 (81.68 kg/h) and an evaporation rate of 2.0 mm/day, a pond area of about 980 m<sup>2</sup> will be necessary.

The brine leaving Step 3 has small amounts of NaCl and KCl and CaSO<sub>4</sub>, therefore upon further processing (above a brine density of 1.354 g/cm<sup>3</sup>) mainly magnesium and calcium salts are expected to crystallize, so this option is not pursued.

The total KCl recovery from the solar pond is 69%, consisting of 54% in the step 1 plus 15% in Step 3. The KCl obtained in Step 1 is not recovered due to the low KCl content in relation to the NaCl content. Considering a KCl recovery of 70%, an on-stream factor of 90% to process the salts in an industrial KCl Plant, for a calculation basis of one ton of KCl 60% K<sub>2</sub>O, the plant will result in about 22.5 ton of solid residues, 10.6 m<sup>3</sup> of bittern brine, 82 ton of evaporated water and an area of 73 m<sup>2</sup> of solar pond.

#### 4. Conclusions

Experimental solubility data for various electrolyte systems were obtained and compared to Pitzer and Harvie's model [5,8] predictions at 20 °C. The Pitzer and Harvie's model agrees well with literature data on the binary systems (NaCl–H<sub>2</sub>O, KCl–H<sub>2</sub>O, MgCl<sub>2</sub>–H<sub>2</sub>O) and ternary systems (NaCl–KCl–H<sub>2</sub>O) at 20 °C considered in this study. The experimental data on the quinary system NaCl–KCl–MgCl<sub>2</sub>–CaCl<sub>2</sub>–H<sub>2</sub>O also compared well with the Pitzer and Harvie's model for brine densities

up to 1.350 kg/m<sup>3</sup>. The model was used to design a fractional crystallization process with three evaporation steps. We have shown that the model is useful for solubility prediction of complex systems and also supply a theoretical basis for the extraction of salts from naturally complex occurring brines.

#### Conflicts of interest

The authors declare no conflicts of interest.

#### Acknowledgments

Authors would like to thank Vale S.A., especially Patrice Mazzone and Keila Gonçalves for authorizing the publication of this work; Nancy Parada, Consultant of Chemicals from Brines for participating in the study for the project involving production of potassium chloride from natural brine. CNPq and CAPES (Brazilian Council for Scientific and Technological Development) are also acknowledged.

#### REFERENCES

- [1] Yang J, Peng J, Duan Y, Tian C, Ping M. The phase diagrams and Pitzer model representations for the system KCl + MgCl<sub>2</sub> + H<sub>2</sub>O at 50 and 75 °C. *Russ J Phys Chem* 2012;1930–5.
- [2] Zuvic P, Parada N, Vergara L. Recovery of potassium chloride, potassium sulfate and boric acid from the Salar de Atacama Brine Sixth International Symposium on Salts, vol. II; 1983.
- [3] Song P, Yao Y. *Calphad* 2003;27:343–52.
- [4] Harvie C, Weare JH. The prediction of mineral solubilities in natural waters: the Na–K–Mg–Ca–Cl–SO<sub>4</sub>–H<sub>2</sub>O system from zero to high concentration at 25 °C. *Geochim Cosmochim Acta* 1980;44:981–97.
- [5] Harvie C, Eugster H, Weare J. Mineral equilibria in the six-component seawater system, Na–K–Mg–Ca–SO<sub>4</sub>–Cl–H<sub>2</sub>O at 25 °C II: compositions of the saturated solutions. *Geochim Cosmochim Acta* 1982;46:1603.
- [6] Harvie C, Moller N, Weare J. The prediction of mineral solubilities in natural waters: the Na–K–Mg–Ca–H–Cl–SO<sub>4</sub>–OH–HCO<sub>3</sub>–CO<sub>3</sub>–CO<sub>2</sub>–H<sub>2</sub>O system to high ionic strengths at 25 °C. *Geochim Cosmochim Acta* 1984;48:723–51.
- [7] Marion GM, Farren RE. Mineral solubilities in the Na–K–Mg–Ca–Cl–SO<sub>4</sub>–H<sub>2</sub>O system: a re-evaluation of the

- sulfate chemistry in the Spencer-Møller-Weare model. *Geochim Cosmochim Acta* 1999;63(9):1305-18.
- [8] Pabalan RT, Pitzer K. Thermodynamics of concentrated electrolyte mixtures and the prediction of mineral solubilities to high temperatures for mixtures in the system Na-K-Mg-Cl-SO<sub>4</sub>-OH-H<sub>2</sub>O. *Geochim Cosmochim Acta* 1987;51:2429-43.
- [9] Spencer R, Moller N, Weare J. The prediction of mineral solubilities in natural waters: a chemical equilibrium model for the Na-K-Ca-Mg-Cl-SO<sub>4</sub>-H<sub>2</sub>O system at temperatures below 25 °C. *Geochim Cosmochim Acta* 1990;54:575-90.
- [10] Butler JN. *Ionic equilibrium a mathematical approach*. London: Addison-Wesley Publishing Company, Inc.; 1964.